

# ***GPS Carrier-Phase Point Positioning with Precise Orbit Products***

P. Héroux, J. Kouba, P. Collins and F. Lahaye  
Natural Resources Canada  
Geodetic Survey Division  
615, Booth Street, Room 458A  
Ottawa, Ontario K1A 0E9  
Canada

## **BIOGRAPHIES**

Pierre Héroux, François Lahaye and Paul Collins are Research Officers in the Active Control Systems Section, Geodetic Survey Division of Geomatics Canada, Natural Resources Canada.

Jan Kouba is actively retired from the Active Control Systems Section, Geodetic Survey Division of Geomatics Canada, Natural Resources Canada.

## **ABSTRACT**

Precise satellite orbits and clocks from the International GPS Service (IGS) are becoming available with increased precision and timeliness. Now that Selective Availability (SA) is permanently switched off, these products can satisfy the most demanding GPS users observing at high data rates. With dual-frequency pseudorange and carrier-phase observations, stand-alone GPS users can now consistently achieve, in post-processing and on a global scale, static and kinematic positioning with cm to dm accuracy. This level of accuracy is possible when GPS users take advantage of very precise satellite clock estimates available with the orbits, while accounting for all known systematic effects affecting their observations. This approach is referred to as Precise Point Positioning (PPP). As it does not involve observation differencing, PPP differs from the more traditional differential positioning techniques that require access to observations from one or more ground based reference stations with known coordinates. The Geodetic Survey Division (GSD) of Natural Resources Canada (NRCan) already supports PPP in post-processing mode and is currently enhancing the orbit and clock products of its real-time GPS Corrections (GPS\*C) service by including IGS Ultra-Rapid orbit predictions and processing carrier-phase data from a wide-area network.

This paper describes the PPP processing of undifferenced GPS observations with IGS precise orbit and clock products. The adjustment procedure is summarized and models that must be implemented are specified. Post-processed positioning results in static and kinematic modes indicate that RMS accuracy from 1-10 cm can be achieved in latitude, longitude and height. Tropospheric zenith delays can be recovered with a RMS accuracy of approximately 1 cm and station clock corrections can be recovered with a RMS accuracy of 0.1-0.2 nanoseconds. Using the GPS\*C real-time orbit and clock products, RMS accuracy between 10 and 30cm can be achieved.

## **1. INTRODUCTION**

PPP processing of undifferenced smoothed pseudoranges with fixed precise satellite orbits and clocks has been used by GSD since 1992 (Héroux, 1993). For applications requiring meter level positioning, this approach has satisfied a number of users. By combining precise IGS satellite clocks at 15 min intervals with 30-second tracking data from selected IGS stations with stable atomic clocks, 30-second precise satellite clocks are also produced (Héroux and Kouba, 1995). These products satisfy GPS users observing at high data rates in either static or kinematic modes for applications requiring meter precision. For GPS users seeking to achieve geodetic precision, sophisticated processing software such as GIPSY (Lichten et al., 1995), BERNESE (Rothacher and Mervart, 1996) and GAMIT (King and Bock, 1999) are required. By using the IGS precise orbit products and combining the GPS carrier phase data with reference station observations, geodetic users achieve precise positioning while integrating into the ITRF. Software provided by receiver manufacturers may also be used as long as it allows for the input of station and orbit data in a standard format.

For a number of years, precise point positioning algorithms using undifferenced carrier phase observations have also been available in the GIPSY GPS analysis software (Zumberge et al., 1997). More recently, they have been added to the traditional double-differencing BERNES software. Users now have the option of processing data from a single station to obtain positions with cm precision within the reference frame provided by the IGS orbit products. NRCan PPP software has also evolved from its original version (H roux et al., 1993) to provide increasing precision. PPP eliminates the need to acquire simultaneous tracking data from a reference (base) station or a network of stations. It has given rise to centralized geodetic positioning services that require from the user the simple submission of a request and valid GPS observation file (Zumberge, 1999). The approach presented here is an implementation of PPP that effectively distributes processing by providing portable software that can be used on a personal computer and takes advantage of the highly accurate global reference frame made available through the IGS orbit products.

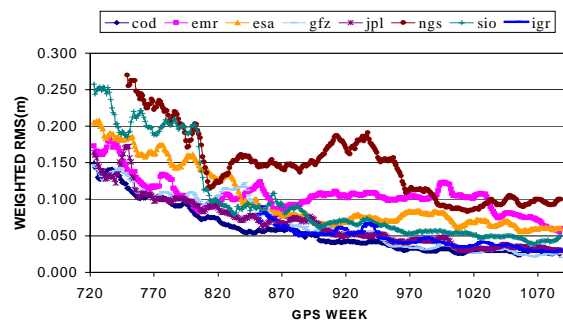
## 2. INTERNATIONAL GPS SERVICE (IGS) ORBIT PRODUCTS

The IGS Precise Orbit products come in three flavors; the Final, Rapid and Ultra-Rapid that differ mainly by their varying accuracy and latency resulting from the extent of the tracking network used for their computation. The IGS Final orbits are combined from 7 contributing IGS Analysis Centers (ACs) and are usually available on the eleventh day after the last observation. The Rapid orbit product is combined 17 hours after the end of the day of interest. The latency is due to orbit computation time and delays in the delivery of 24-hour tracking data files from stations of the global IGS tracking network. Recently, Data Centers have been asked to forward hourly tracking data to accelerate product delivery. This new submission scheme was required for the creation of an Ultra-Rapid product, with a latency of only a few hours, to satisfy the more demanding needs of the meteorological community and future LEO (Low Earth Orbiter) missions. It is expected that IGS products will continue to be delivered with increased timeliness in the future (Neilan et al., 1997, Kouba et al., 1998).

The IGS Final product is the most accurate GPS orbit available. Over the past 8 years (Figure 1), the quality of the IGS Final orbits has improved from about 30 cm to the 3-5 cm precision level currently realized by some of the AC's (Kouba, 1998). It is also interesting to note that the Rapid orbit combined product is as precise as the best AC Final solution with less tracking stations and faster delivery time (17 hours). This fact confirms the belief that increasing the number of global GPS tracking stations does not necessarily translate into higher orbit precision. Finally, the Ultra-Rapid product, delivered twice daily with 3 hour latency, compares favourably to the Rapid in its estimated portion and contains a predicted 24-hour segment for real-time usage.

One element that has not yet received much attention is the quality of the GPS satellite clock estimates included in the IGS orbit products. Examining the IGS Final summary reports (<http://igscb.jpl.nasa.gov/mail/igsreports/>) produced weekly by the IGS AC coordinator, we notice that satellite clock estimates produced by different AC's agree within 0.1-0.2 nanosecond RMS, or 3-6 cm, a level which is compatible with the orbit precision. The combination of precise GPS orbits and clocks weighted according to their respective uncertainties, is essential for PPP, given that proper measurements are made by the user and the observation models are correctly implemented.

Figure 1: Weighted Orbit RMS of the IGS Rapid and AC Final orbit solutions with Respect to the IGS Final Orbit Products



### 3. UNDIFFERENCED CODE/CARRIER PROCESSING

#### 3.1. UNDIFFERENCED CODE/CARRIER OBSERVATION EQUATIONS

The ionospheric-free combinations of dual-frequency GPS pseudorange ( $P$ ) and carrier-phase observations ( $\Phi$ ) are related to user position, clock, troposphere and ambiguity parameters according to the following simplified observation equations:

$$\ell_P = \rho + C(dt - dT) + M ztd + \varepsilon_P \quad (1)$$

$$\ell_\Phi = \rho + C(dt - dT) + M ztd + N \lambda + \varepsilon_\Phi \quad (2)$$

where:

$\ell_P$  is the ionosphere-free combination of L1 and L2 pseudoranges ( $2.54P_1 - 1.54P_2$ ),

$\ell_\Phi$  is the ionosphere-free combination of L1 and L2 carrier-phases ( $2.54\phi_1 - 1.54\phi_2$ ),

$\rho$  is the geometrical range between satellite ( $X_s, Y_s, Z_s$ ) and station ( $x, y, z$ ),

$C$  is the vacuum speed of light,

$dt$  is the station clock offset from GPS time,

$dT$  is the satellite clock offset from GPS time,

$M$  is function to map tropospheric from slant to zenith,

$ztd$  is the signal tropospheric zenith total delay due to the neutral-atmosphere,

$\lambda$  is the carrier, or carrier-combination, wavelength,

$N$  is the ambiguity of the carrier-phase ionosphere-free combination, and

$\varepsilon_P, \varepsilon_\Phi$  are the relevant measurement noise components, including multipath.

Geometric range  $\rho$  is a function of satellite ( $X_s, Y_s, Z_s$ ) and station ( $x, y, z$ ) coordinates according to:

$$\rho = \sqrt{(X_s - x)^2 + (Y_s - y)^2 + (Z_s - z)^2}$$

#### 3.2. PRECISE POINT POSITIONING ADJUSTMENT MODEL

Given precise estimates of GPS satellite orbits and clocks, equations (1) and (2) reduce to:

$$\ell_P = \rho + C dt + M ztd + \varepsilon_P \quad (3)$$

$$\ell_\Phi = \rho + C dt + M ztd + N \lambda + \varepsilon_\Phi \quad (4)$$

Linearization of observation equations (3) and (4) around the a-priori parameters and observations ( $X^0, \ell$ ) becomes, in matrix form:

$A \delta + W - V = 0$ , where  $A$  is the design matrix,  $\delta$  is the vector of corrections to the unknown parameters  $X$ ,  $W = f(X^0, \ell)$  is the misclosure vector and  $V$  is the vector of residuals.

The partial derivatives of the observation equations with respect to the vector of unknown parameters  $X$ , containing station position ( $x, y, z$ ), clock ( $dt$ ), troposphere zenith total delay ( $ztd$ ) and real-valued carrier-phase ambiguities ( $N$ ), form the design matrix  $A$ . The least squares solution with a-priori weighted parameter constraints ( $P_x$ ) is given by:

$$\delta = -(P_{X^0} + A^T P_\ell A)^{-1} A^T P_\ell W,$$

so that the estimated parameters are

$$\hat{X} = X^0 + \delta,$$

with covariance matrix

$$C_{\hat{X}} = P_{\hat{X}}^{-1} = (P_{X^0} + A^T P_\ell A)^{-1}.$$

#### 3.3. PRECISE POINT POSITIONING ADJUSTMENT PROCEDURE

The adjustment procedure developed is effectively a sequential filter that adapts to varying user dynamics. The implementation considers the variations in the states of the parameters between observation epochs and uses appropriate stochastic processes to update their variances.

Using subscript  $i$  to denote a specific time epoch, we see that without observations between epochs, initial parameter estimates at epoch  $i$  are equal to the ones obtained at epoch  $i-1$ :

$$X_i^0 = \hat{X}_{i-1}.$$

To propagate the covariance information from epoch  $i-1$  to  $i$ , during an interval  $\Delta t$ ,  $C_{\hat{x}_{i-1}}$  has to be updated to include process noise represented by the covariance matrix  $C\varepsilon_{\Delta t}$ :

$$P_{X_i^0} = [C_{\hat{x}_{i-1}} + C\varepsilon_{\Delta t}]^{-1}$$

Process noise can be adjusted according to user dynamics, receiver clock behaviour and atmospheric activity. In all instances, the process noise assigned to the ambiguity parameters  $C\epsilon(N^j_{(j=1,nsat)})_{\Delta t} = 0$ , since the carrier-phase ambiguities remain constant over time. In static mode, the user position is also constant and consequently  $C\epsilon(x)_{\Delta t} = C\epsilon(y)_{\Delta t} = C\epsilon(z)_{\Delta t} = 0$ . In kinematic mode, it is increased as a function of user dynamics. The receiver clock process noise can vary as a function of frequency stability but is usually set to white noise with a large  $C\epsilon(dt)_{\Delta t}$  value to accommodate the unpredictable occurrence of clock resets. A random walk process noise of 5 mm/ $\sqrt{\text{hour}}$  is usually assigned to the zenith path delay  $C\epsilon(ztd)_{\Delta t}$ .

#### 4. UNDIFFERENCED PROCESSING CORRECTION MODELS

When attempting to combine satellite orbits and clocks precise to a few cms with ionospheric-free carrier phase observations (with mm resolution), it is important to account for some effects that may be neglected in differential phase processing. Satellite attitude and site correction models that are significant for carrier phase point positioning are summarized below and explained in detail in (Kouba, et al., 2000). A number of the corrections listed below require the Moon or the Sun positions which can be obtained from readily available planetary ephemerides files, or more conveniently from simple formulas (as implemented here) since a relative precision of about 1/1000 is sufficient for corrections with mm precision. Note that for cm level differential positioning and baselines of less than 100 km, the correction terms discussed below can be safely neglected.

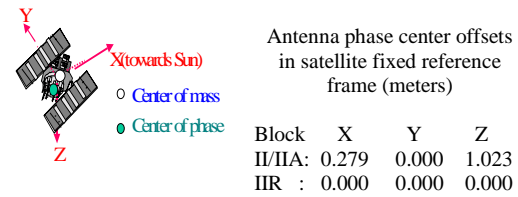
##### 4.1. SATELLITE ATTITUDE EFFECTS

###### 4.1.1. SATELLITE ANTENNA OFFSETS

The requirement for satellite based corrections originates from the separation between the GPS satellite center of mass and the phase center of its antenna. Because the force models used for satellite orbit modeling refer to its center of mass, the IGS GPS precise satellite coordinates and clock products also refer to the satellite center of mass, unlike the orbits broadcast in the GPS navigation message that refer to satellite antenna phase center. Since the measurements

are made to the antenna phase center, one must use known or conventional satellite phase center offsets and monitor the orientation of the offset vector in space as the satellite orbits the Earth. The phase centers for most satellites are offset both in the body z coordinate direction (towards the Earth) and in the body x coordinate direction which is on the plane containing the Sun (see Figure 2).

**Figure 2: IGS Conventional Antenna Phase Center in Satellite Fixed Reference Frame (in meters)**



###### 4.1.2. PHASE WIND-UP

GPS satellites transmit right circularly polarized (RCP) radio waves and therefore, the observed carrier-phase depends on the mutual orientation of the satellite and receiver antennas. A rotation of either receiver or satellite antenna around its bore axis will change the carrier-phase up to one cycle (one wavelength), which corresponds to one complete revolution of the antenna. This effect is called “phase wind-up” (Wu et al., 1993). A receiver antenna, unless mobile, does not rotate and it is oriented towards a reference direction (usually north). However, satellite antennas undergo slow rotations as their solar panels are being oriented towards the Sun and the station-satellite geometry changes.

The phase wind-up correction has been generally neglected even in the most precise differential positioning software, as it is quite negligible for double difference positioning on baselines/networks spanning up to a few hundred kilometers. Although, it has been shown that it can reach up to 4 cm for a baseline of 4000 km (Wu et al., 1993). This effect is quite significant for undifferenced point positioning when fixing IGS satellite clocks since it can reach up to one half of the wavelength. Neglecting it and fixing IGS orbits/clocks will result in position and clock errors at the dm level. For receiver antenna rotations (e.g. during kinematic positioning/navigation) phase wind-up is fully absorbed into the station clock solutions.

#### 4.1.3. NOON AND MIDNIGHT TURNS

In addition to the gradual phase wind-up, satellites are also subject to rapid rotations during eclipsing seasons, called “noon” and “midnight” turns, that reorient their solar panels towards the Sun. This can represent antenna rotations of up to one revolution within less than half an hour. During such noon or midnight turns, phase data needs to be corrected (Bar-Sever, 1992) or edited out.

### 4.2. SITE DISPLACEMENT EFFECTS

In a global sense, a station undergoes real or apparent periodic movements reaching a few dm that are not included in the corresponding ITRF position. Consequently, if one is to obtain a precise station coordinate solution consistent with the current ITRF conventions, these station movements must be modelled by adding the site displacement correction terms listed below to the conventional ITRF coordinates. Effects with magnitude of less than 1 cm such as atmospheric and snow build-up loading have not been considered in the following.

#### 4.2.1. SOLID EARTH TIDES

The “solid” Earth is in fact pliable enough to respond to the same gravitational forces that generate the ocean tides. The periodic vertical and horizontal site displacements caused by tides are represented by spherical harmonics of degree and order ( $n$   $m$ ) characterized by the Love number  $h_{nm}$  and the Shida number  $l_{nm}$ . The effective values of these numbers weakly depend on station latitude and tidal frequency (Wahr, 1981) and need to be taken into account when an accuracy of 1 mm is desired in determining station positions (see e.g. IERS Conventions (IERS, 1996)). For 5 mm precision, only the second degree tides, supplemented with a height correction term are necessary.

The tidal correction can reach about 30 cm in the radial and 5 cm in the horizontal direction. It consists of a latitude dependent permanent displacement and a periodic part with predominantly semi diurnal and diurnal periods of changing amplitudes. The periodic part is largely averaged out for static positioning over a 24-hour period. However, the permanent part, which can reach up to 12 cm in mid latitudes (along the radial direction) remains in such a 24h

average position. Even when averaging over long periods, neglecting the tidal correction in point positioning would result in systematic position errors of up to 12.5 and 5 cm in the radial and north directions, respectively. Note that for differential positioning over short baseline (<100km), both stations have almost identical tidal displacements so that the relative positions over short baselines will be largely unaffected by the solid Earth tides.

#### 4.2.2. ROTATIONAL DEFORMATION DUE TO POLAR MOTION (POLAR TIDES)

Much like deformations due to the Sun and Moon, attractions that cause periodical station position deformations, the changes of the Earth’s spin axis with respect to Earth’s crust, i.e. the polar motion, causes periodical deformations due to minute changes in the Earth centrifugal potential. Using the above second degree Love and Shida numbers, the corrections to latitude, longitude (+east) and height can be computed (IERS, 1996). Since most ACs are utilizing this correction when generating their orbit/clock solutions, the IGS combined orbits/clocks are consistent with these station position corrections. For sub-cm position accuracy, the above polar tide corrections need to be applied to obtain an apparent station position, or alternatively subtracted from the position solutions to be consistent with ITRF. Unlike the solid earth tides and the ocean loading effects, the pole tides do not average to zero over a 24-hour period. They depend on station position and vary slowly according to the polar motion with predominant seasonal and Chandler periods. The maximum polar tide displacements can reach about 25 mm in the height and about 7 mm in the horizontal directions.

#### 4.2.3. OCEAN LOADING

Ocean loading is similar to solid Earth tides in that it is dominated by diurnal and semi diurnal periods, but it results from the load of the ocean tides. While ocean loading is almost an order of magnitude smaller than solid Earth tides, it is more localized and by convention it does not have a permanent part. For single epoch positioning at the 5 cm precision level, or mm static positioning over 24h period and/or for stations that are far from the oceans, ocean loading can be safely neglected. On the other hand, for cm precise kinematic point positioning or precise static positioning along coastal regions

over intervals significantly shorter than 24h, this effect has to be taken into account. Note that when the tropospheric ztd or clock solutions are required, the ocean load effects also have to be taken into account even for a 24h static point positioning processing, unless the station is far ( $> 1000$  km) from the nearest coast line. Otherwise, the ocean load effects will map into the tropospheric ztd/clock solutions (Dragert, 2000), which may be significant particularly for the coastal stations. The ocean load effects can be modeled in each principal direction by correction terms found in IERS Conventions (IERS, 1996).

#### **4.2.4. SUB-DAILY EARTH ROTATION PARAMETERS**

The IGS orbit products imply the underlying ERP. Consequently, IGS users who fix or heavily constrain the IGS orbits and work directly in ITRF need not be concerned about ERP. For point positioning processing formulated within the terrestrial frame, with the IGS orbits held fixed, the so called sub-daily ERP model, which is also dominated by diurnal and sub-diurnal periods of ocean tide origin, is still required to attain sub cm positioning precision. This results from the IERS convention for ERP, i.e. the IERS/IGS ERP series as well as ITRF positions do not include the sub-daily ERP variations, which can reach up to 3 cm at the surface of the earth. However, the IGS orbits imply the complete ERP, i.e. the conventional ERP plus the sub-daily ERP model. In order to be consistent, in particular for precise static positioning over intervals much shorter than 24 h, this sub-daily effect needs to be taken into account. Note that much like the ocean tide loading, the sub-daily ERP are averaged out to nearly zero over a 24h period.

#### **4.2.5. OTHER CONSIDERATIONS**

Selection of an antenna with known antenna phase center variations as a function of the azimuth and elevation of the incoming GPS signal is necessary and must be applied. The location of the phase center of a GPS antenna can vary by as much as 2 cm as a function of the azimuth and elevation of the incoming satellite signal. A table of elevation dependent relative antenna phase center variations with respect to an adopted standard has been compiled by the IGS and includes values from field calibrations for most models of antennas used for precise

applications. It has also been observed and reported that the addition of radomes for antenna protection can significantly affect phase center variations.

Finally, if station clock solutions are required, a specific set of pseudorange observations consistent with the IGS clock products needs to be used otherwise the clock solutions are significantly affected. This is a result of significant satellite dependent differences between L1 C/A ( $P_{CA}$ ) and P ( $P_I$ ) code pseudoranges which can reach up to 2 ns (60 cm).

### **5. PRECISE POINT POSITIONING POST-PROCESSING RESULTS**

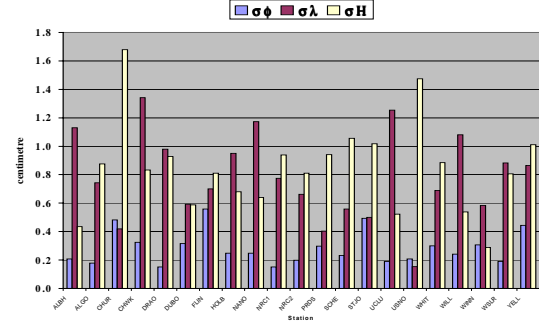
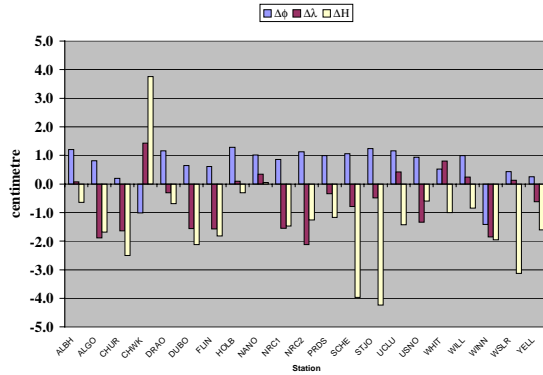
#### **5.1. STATIC PPP PROCESSING**

Since January 1, 2001, 24-hour sessions from approximately 20 continuously operating GPS tracking stations in Canada have been processed daily with PPP using IGS rapid orbit/clock product. Observations every 15 minutes are processed, the times for which precise orbits/clocks are available in the final (IGS) and rapid (IGR) SP3 files. Daily differences in latitude, longitude and height with respect to epoch ITRF coordinates are computed to evaluate the precision of PPP daily estimates. Table 1 and Figure 3 show for GPS week 1111 (April 22-28,2001), the weekly average station coordinate differences ( $\Delta\phi$ ,  $\Delta\lambda$ ,  $\Delta H$ ) and their standard deviation over 7-days ( $\sigma\phi$ ,  $\sigma\lambda$ ,  $\sigma H$ ). These results show that PPP in static mode using 24-hour data sets and IGS or IGR orbits is in agreement with ITRF epoch values at the sub-cm level in the horizontal components and at 1-2 cm in the vertical. The standard deviations show sub-cm day-to-day repeatability in all components for most stations.

**Table 1: Static PPP Mean Coordinate Differences and Standard Deviations, GPS Week 1111**

(cm)	IGS						IGR					
Station	$\Delta\phi$	$\Delta\lambda$	$\Delta H$	$\sigma\phi$	$\sigma\lambda$	$\sigma H$	$\Delta\phi$	$\Delta\lambda$	$\Delta H$	$\sigma\phi$	$\sigma\lambda$	$\sigma H$
ALBH	1.2	0.1	-0.6	0.2	1.1	0.4	1.4	0.7	-1.1	0.3	0.9	0.5
ALGO	0.8	-1.9	-1.7	0.2	0.7	0.9	0.7	-1.7	-1.1	0.3	0.8	0.9
CHUR	0.2	-1.6	-2.5	0.5	0.4	1.7	0.2	-1.0	-1.9	0.5	0.6	1.3
CHWK	-1.0	1.4	3.8	0.3	1.3	0.8	-0.8	2.1	3.1	0.3	0.8	0.8
DRAO	1.2	-0.3	-0.7	0.2	1.0	0.9	1.4	0.4	-1.0	0.2	0.6	0.6
DUBO	0.6	-1.6	-2.1	0.3	0.6	0.6	0.5	-0.9	-1.5	0.4	0.9	0.9
FLIN	0.6	-1.6	-1.8	0.6	0.7	0.8	0.7	-0.8	-1.2	0.4	0.5	0.7
HOLB	1.3	0.1	-0.3	0.2	1.0	0.7	1.6	0.8	-1.1	0.3	0.5	0.8
NANO	1.0	0.3	0.1	0.2	1.2	0.6	1.3	0.8	-0.6	0.3	0.6	0.9
NRC1	0.9	-1.5	-1.5	0.2	0.8	0.9	0.7	-1.4	-0.9	0.2	0.8	1.1
NRC2	1.1	-2.1	-1.3	0.2	0.7	0.8	1.0	-1.9	-0.7	0.2	0.7	1.1
PRDS	1.0	-0.3	-1.2	0.3	0.4	0.9	1.1	0.2	-1.2	0.2	0.4	1.0
SCHE	1.1	-0.8	-4.0	0.2	0.6	1.1	0.9	-0.7	-3.4	0.2	0.8	1.1
STJO	1.2	-0.5	-4.2	0.5	0.5	1.0	1.0	-0.4	-3.8	0.5	0.3	1.0
UCLU	1.2	0.4	-1.4	0.2	1.3	0.5	1.4	1.0	-2.2	0.1	1.0	0.5
USNO	0.9	-1.3	-0.6	0.2	0.2	1.5	0.9	-1.9	-0.3	0.3	1.0	1.5
WHIT	0.5	0.8	-1.0	0.3	0.7	0.9	1.1	1.1	-1.8	0.3	0.4	0.4
WILL	1.0	0.2	-0.8	0.2	1.1	0.5	1.2	0.9	-1.0	0.2	0.8	0.6
WINN	-1.4	-1.9	-2.0	0.3	0.6	0.3	-1.4	-1.3	-1.6	0.3	0.8	0.8
WSLR	0.4	0.1	-3.1	0.2	0.9	0.8	0.7	0.7	-3.5	0.3	0.5	0.8
YELL	0.3	-0.6	-1.6	0.4	0.9	1.0	0.7	0.1	-1.3	0.3	0.7	0.7
Mean	0.7	-0.6	-1.4	0.3	0.8	0.8	0.8	-0.2	-1.3	0.3	0.7	0.9

**Figure 3: Static PPP Day-to-day Repeatability, Week 1111**



## 5.2. STATION ZENITH TROPOSPHERIC DELAY

The PPP approach solves for station zenith tropospheric delays (ZTD). Using precise orbits and clocks at 15-minute intervals, ZTD estimates for all Canadian sites during GPS week 1111 were obtained. To assess their quality, selected sites with available IGS combined ZTD estimates (Gendt, 1998) were used for inter-comparison. The IGS produces weekly files of combined ZTD estimates at 2-hour interval for more than 100 globally distributed sites since 1997. Station ZTD estimates are by-products of the IGS Analysis Center processing aimed mainly at solving GPS satellite orbits, station coordinates and global geophysical parameters. Therefore, the number of global sites for which IGS ZTD estimates are available is limited since IGS ACs generally only process between 30 and 100 global stations. The ZTD consistency between the IGS AC estimates and the combined mean is at the 4 mm level (Gendt, 1998). Absolute accuracy of GPS-derived precipitable water-vapor (PWV) estimates have been obtained by comparison to water vapor radiometer (WVR) measurements at collocated sites and show agreement at the 1 mm level (translates to ~7mm ZTD). Comparisons with radiosonde data show similar level of agreement (Seglenieks, 2001).

Figure 4 shows the IGS and PPP ZTD time series at 2-hour interval during GPS week 1111 (day of year 112-118). The agreement is evident as summarized in Table 2, with 5-mm maximum weekly average difference and sub-cm standard deviations.

**Figure 4: IGS and PPP ZTD Estimates, Week 1111, Stations ALGO, DRAO, YELL, STJO**

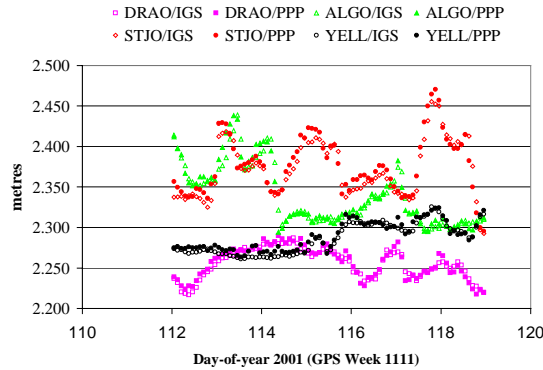


**Table 2. ZTD Mean Differences and Standard Deviations, PPP- IGS Combined, GPS Week 1111**

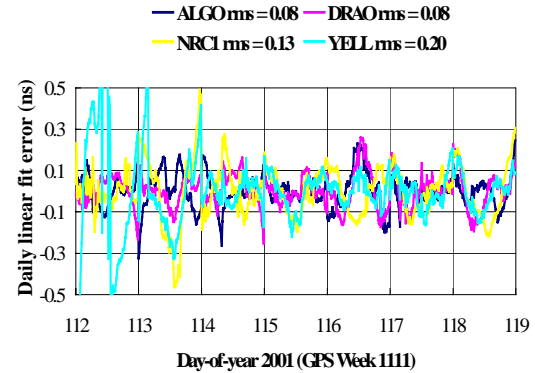
Station	$\Delta$ ZTD(mm)	$\sigma$ ZTD(mm)
ALGO	0.9	9.2
DRAO	1.6	5.7
STJO	4.6	9.9
YELL	3.7	4.8

### 5.3. STATION CLOCK

The PPP approach also solves for the GPS receiver clock, be it internal or external. Assessing the quality of the PPP clock determinations is difficult due to the absence of a quality absolute standard for comparison. Nevertheless, with GPS receivers connected to external Hydrogen Maser (HM) frequency standards at stations such as DRAO, YELL, ALGO and NRC1, it is possible to assess the quality of the daily PPP clock estimates. This is done by considering the residuals from a linear regression on the PPP receiver clock estimates, assuming that the HM have a stable and constant frequency offset (linear clock drift) over 24-hours.

The 15-minute receiver clock residuals after a daily linear regression for the 7-days of GPS week 1111 are presented on Figure 5. The RMS of the clock residuals are at the 0.0-0.2 nanosecond level (3-6 cm), which is compatible with the quality of the GPS satellite clocks in the IGS rapid and final orbit products. Departures that reach the .5 ns level on days 112 and 113 at YELL are caused by poor geometry resulting from receiver tracking problems.

**Figure 5: PPP Receiver Clock Residuals, Week 1111, Stations ALGO, DRAO, NRC1, YELL**



### 5.4. KINEMATIC POINT POSITIONING

PPP can also be used in kinematic mode to process GPS data collected under various user dynamics. By adding process noise to station coordinate parameters between observation epochs, the static positioning model is easily adapted for single receiver kinematic applications. In post-processing, back-substitution (smoothing) gives optimal results. Kinematic PPP was evaluated with data from GPS week 1111 collected in static mode at stations ALGO, DRAO, STJO and YELL. While the GPS data collected in static mode does not exactly reflect all of the conditions a GPS receiver may experience under truly dynamic conditions, the quality of the position estimates is equivalent, given appropriate data quality and continuity and sufficient GPS satellite geometry.

Results presented in Table 3 represent the positioning precision that can be achieved in kinematic PPP. Of the 4 stations included, we see that horizontal and vertical precisions of 5 and 10 cm respectively were realised during GPS week 1111 at all sites except Yellowknife. Figures 6 and 7 show in more detail the epoch position determinations at 15-minute intervals over the 7-day period, with associated precision estimates. These figures show clearly that the errors are compatible with the level of uncertainty assigned to the positions, indicating that observation quality or GPS satellite geometry is the root cause of the errors. This reflects the vulnerability of the kinematic PPP



solution to GPS carrier phase observation quality and continuity, since it estimates carrier phase ambiguities. When frequent data outages or phase discontinuities occur at a station such as YELL, the positioning quality is degraded.

**Table 3: Kinematic PPP Mean Coordinate Differences and Standard Deviations, GPS Week 1111**

(cm)	$\Delta\phi$	$\Delta\lambda$	$\Delta H$	$\sigma\phi$	$\sigma\lambda$	$\sigma H$
ALGO	-0.5	-0.2	0.5	4.6	4.1	10.4
DRAO	-0.2	-0.9	-2.7	5.6	3.4	6.9
STJO	0.2	-3.3	-0.1	7.6	7.4	13.1
YELL	3.4	0.3	-0.2	18.3	10.4	47.2

**Figure 6: PPP Kinematic Positioning, Week 1111, Station DRAO**

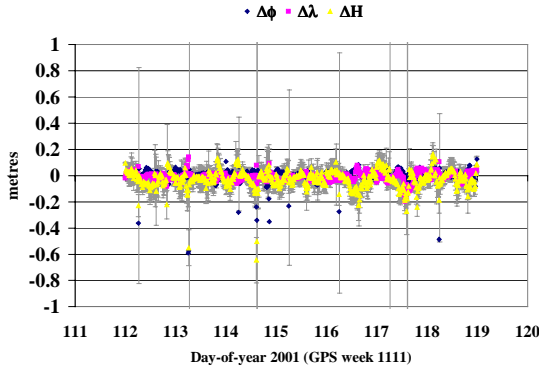
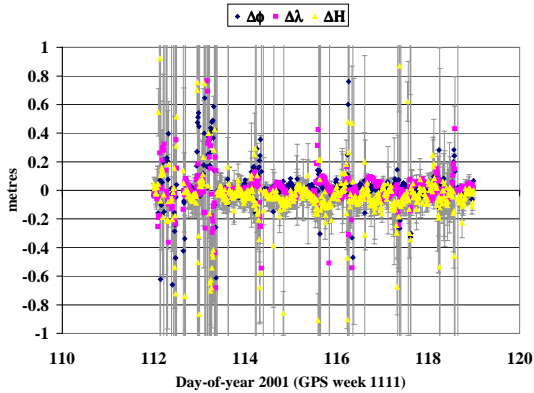


**Figure 7: PPP Kinematic Positioning, Week 1111, Station YELL**



## 6. REAL-TIME WIDE-AREA CARRIER PHASE PROCESSING

Having realised the potential of PPP in post-processing, GSD is currently enhancing its

implementation of real-time Wide Area Differential GPS (WADGPS) with carrier phase processing. This development is aimed at improving the quality of GPS satellite clock corrections to facilitate real-time carrier phase PPP. By-products of this development are precise estimates of station clocks and tropospheric zenith delays both at the wide-area reference stations, and potentially at any user's site.

Preliminary results indicate that tropospheric zenith delays can be recovered with an RMS accuracy of approximately one cm, station clock corrections can be recovered with an RMS accuracy of 0.1-0.2 nanoseconds, and satellite clock corrections can be recovered with an RMS accuracy of approximately one nanosecond. Positioning tests with dual frequency data produced RMS accuracies between 10 and 30cm in latitude, longitude and height (Collins, 2001).

## 7. CONCLUSION

The observation equations, estimation technique and correction models used for GPS PPP using IGS orbit/clock products were described. Results from daily post-processing of station dual-frequency pseudorange and carrier phase observations from stationary GPS receivers at 20 Canadian sites show cm positioning precision and sub-cm day-to-day repeatability. Furthermore, station tropospheric zenith path delays with cm precision are recovered as well as GPS receiver clock estimates precise to 100 ps. Kinematic PPP was also applied to data sets from stationary GPS receivers showing cm to dm single epoch positioning precision depending only on data quality, continuity and GPS satellite geometry. PPP reliance on the carrier phase observable and the ability to solve ambiguities makes it vulnerable to data outages, a familiar condition experienced by users of differential carrier phase processing techniques. While results presented herein used IGS orbits/clocks at 15 minute intervals, it is worth noting that IGS now produces 5-min IGS combined satellite clocks daily. Since the decommissioning of Selective Availability (SA) in May 2000, these clocks can be interpolated with cm-dm precision (Zumberge and Gent, 2000) and used to process GPS data observed at any sampling interval to achieve cm to dm static and kinematic positioning, without reference or base station data.

Comparable results were obtained with IGS rapid and final orbit products, meaning that these precisions are presently available within 24 hours of data collection. The challenge now is to bring GPS PPP capability to real-time. GSD is currently working towards a wide-area carrier-phase processing strategy that will provide real-time GPS orbits and clocks with cm precision.

## 8. ACKNOWLEDGMENTS

The authors are grateful to the Geodetic Survey Division staff who operate maintain the GPS stations that form the Canadian Active Control System and to the many individuals and organizations worldwide who contribute to the International GPS Service. IGS data and products are the result of an unprecedented voluntary, yet coordinated effort that continues to provide an invaluable service to the scientific and GPS positioning communities.

## 9. REFERENCES

- Bar-Sever, Y. E. (1996), A New Model for GPS Yaw Attitude, *Journal of Geodesy*, 70, pp 714-723.
- Collins, P., F. Lahaye, J. Kouba and P. Héroux (2001). "Real-Time WADGPS Corrections from Undifferenced Carrier Phase". Proceedings of the National Technical Meeting, January 22-24, Long Beach, Calif. pp. 254-260.
- Dragert, H., T.S. James, and A. Lambert (2000). Ocean Loading Corrections for Continuous GPS: A Case Study at the Canadian Coastal Site Holberg, *Geophysical Research Letters*, Vol. 27, No. 14, pp. 2045-2048, July 15.
- Gendt, G. (1998). IGS Combination of Tropospheric Estimates – Experience from Pilot Experiment, Proceedings of 1998 IGS Analysis Center Workshop, J.M. Dow, J. Kouba and T. Springer, Eds. IGS Central Bureau, Jet Propulsion Laboratory, Pasadena, CA, pp. 205-216.
- Héroux, P., M. Caissy, and J. Gallace (1993). Canadian Active Control System Data Acquisition and Validation. Proceedings of the 1993 IGS (International GPS Service for Geodynamics) Workshop, University of Bern, pp. 49-58.
- Héroux, P. and J. Kouba (1995). GPS Precise Point Positioning with a Difference, Paper presented at Geomatics '95, Ottawa, Ontario, Canada, June 13-15.
- IERS (1996). IERS Conventions (1996), IERS Technical Note 21, (ed. D.D. McCarthy)
- King, R. W., and Y. Bock (1999). Documentation of the GAMIT GPS Analysis Software (version 9.8), Unpublished, Massachusetts Institute of Technology, Cambridge, Massachusetts.
- Kouba, J. (1998) IGS Analysis Activities (1998). IGS Annual Report, IGS Central Bureau, Jet Propulsion Laboratory, Pasadena, CA, pp. 13-17.
- Kouba, J. and P. Héroux (2000). "GPS Precise Point Positioning Using IGS Orbit Products." Submitted to *GPS Solutions*.
- Lichten, S.M., Y.E. Bar-Sever, E.I. Bertiger, M. Heflin, K. Hurst, R.J. Muellerschoen, S.C. Wu, T.P. Yunck, and J. F. Zumberge (1995) GIPSY-OASIS II: A High precision GPS Data processing System and general orbit analysis tool, Technology 2006, NASA Technology Transfer Conference, Chicago, Il., Oct. 24-26.
- Neilan, R.E., Zumberge, J.F., Beutler, G., & Kouba, J. (1997). The International GPS Service: A global resource for GPS applications and research. In Proc. ION-GPS-97 (pp. 883-889). The Institute of Navigation.
- Rothacher, M. and L. Mervart (1996). The Bernese GPS Software Version 4.0. Astronomical Institute, University of Berne, Berne, Switzerland.
- Seglenieks<sup>1</sup>, F., C. Smith<sup>2</sup>, B. Proctor<sup>2</sup> and E.D. Soulis<sup>1</sup> (2001). Determination of integrated water vapour using a GPS receiver: Results from Southern Ontario and Fort Smith, <sup>1</sup>Department of Civil Engineering, University of Waterloo, <sup>2</sup>Climate Research Branch, Environment Canada. Presented at CGU 2001, Ottawa, Canada, May 14-17, 2001.
- Wahr, J.M. (1981). The forced nutation of an elliptical, rotating, elastic, and oceanless Earth, *Geophys. J. Roy. Astron. Soc.*, 64, pp. 705-727.

Wu, J.T., S.C. Wu, G.A. Hajj, W.I. Bertiger, and S.M. Lichten (1993). Effects of antenna orientation on GPS carrier phase, , *Manuscripta Geodaetica* 18, pp. 91-98.

Zumberge, J.F., Heflin, M.B., Jefferson, D.C., Watkins, M.M., & Webb, F.H. (1997). Precise point positioning for the efficient and robust analysis of GPS data from large networks. *Journal of Geophysical Research*, 102, 5005-5017.

Zumberge, J.F. (1999). Automated GPS Data Analysis Service. *GPS Solutions*, Vol. 2, No. 3, pp.76-78.

Zumberge, J. and Gent G. (2000),. The Demise of selective availability and implication for the International GPS Service, position paper presented at the IGS Network Workshop, July 10-14, 2000, Oslo, Norway.